Development of a solar-powered device for bloodworm control in rice fields

Ahmed Shawky El-Sayed[1*], Mohamed Mansour Shalaby Refaay[2]

(1. Department of Agricultural Bioengineering Systems, Agricultural Engineering Research Institute (AEnRI), Agricultural Research Center (ARC), Giza 12311, Egypt;

2. Department of Agricultural Operations Mechanization Systems, Agricultural Engineering Research Institute (AEnRI), Agricultural Research Center (ARC), Giza, 12311, Egypt)

Abstract: The aim of this research is to develop a solar-powered device to control the bloodworm *Chironomus spp*. in rice fields instead of using harmful chemical pesticides. The developed control device uses clean solar energy and helps to protect the environment from pesticide pollution residuals. The developed control device generates a continuous high-voltage electrocution current under soil surface to exterminate adult bloodworms and larvae. The device is provided with a fully automated electronic control circuit, an electrocution generator, and a group of electrodes. Three factors were examined to assess the efficacy of the bloodworm control device. Four electrocution potential levels (8, 12, 16, and 20 kV) were tested. Additionally, three electrode depth levels (60, 120, and 180 mm) were examined with three operating periods (10, 20, and 30 minutes). The results show high significance bloodworm population reduction using the developed device, comparing with the chemical insecticide control treatment using *Furadan* (Carbofuran) 10% granular. The reduction percent in bloodworms reached 90.92% and 91.94% in adult bloodworms and larvae, respectively, at the highest levels of the tested variables. The operating costs of the device ranged from 25 to 40 USA $ ha^{-1}, while the consumed energy ranged from 40 to 100 kW h ha^{-1}. The use of the solar-powered control device is effective in exterminating adult bloodworms and their larvae in a short time. So, it is recommended to use the solar-powered control device to exterminate the bloodworm in rice fields.

Keywords: blood worms; electrocution; electrode; pesticide; pitfall trap; sampler.

Citation: El-Sayed, A. S., and M. M. S. Refaay. 2024. Development of a solar-powered device for bloodworm control in rice fields. Agricultural Engineering International: CIGR Journal, 26(3): 58-70.

1 Introduction

Rice is one of the most important strategic crops globally, with about 162 million hectares being cultivated annually. Rice is the main food on the continents of Asia and Africa, where Asia produces about 90% of the global production of rice (Shaheen et al., 2022). In Egypt, the rice crop represents about 22% of the total area cultivated in summer crops (Hegazy et al., 2021). Pests developed biological resistance as a result of pesticide dependency in general, which forces manufacturers of pesticides to use more active ingredients and harms the ecosystem (Liu et al., 2014). Bloodworms reduce the rice seedling numbers with about 95% due to the increased bloodworm population immediately after irrigation, reproduces in only one generation, and must be combated (Stevens et al., 2013). The rice crop's surface irrigation system contributes to spray erosion and soil pesticide absorption. All of these elements contribute to a decline in pest management

Received date: 2023-10-24 **Accepted date:** 2024-03-07

***Corresponding Author: Ahmed Shawky El-Sayed,** Senior Researcher of Department of Agricultural Bioengineering Systems, Agricultural Engineering Research Institute (AEnRI), Agricultural Research Center (ARC), Giza, Egypt. E-mail: a.shawky71@yahoo.com. Tel: 00201065081786.

effectiveness and an increase in soil and water contamination, endangering human health. As a result, environmentally responsible alternative control techniques must be created (Yang et al., 2021). Pesticides used in uncontrolled methods have a direct impact on water pollution, especially in developed countries (Weiss et al., 2022). Flood-irrigated crops, such as rice, are exposed to infection by a group of dangerous pests, such as bloodworms. Infection with bloodworms reduces the quantity and quality of the rice crop (Savary et al., 2019; Sarwar, 2020). Agricultural treatments to minimize the insect population, including the establishment of integrated pest control management systems employing modern techniques, are necessary to lessen the economic damage caused by pests to the rice crop (Montauban et al., 2021).

To eliminate bloodworms, farmers are forced to use chemical pesticides with long residual effects, resulting in poor-quality rice (Kamara, 2015). Bloodworm infection increases the number of bacterial infections that injure crops like rice because the worms secrete mucus that encourages bacterial growth and causes numerous root diseases (Gudeta et al., 2021). Environmentally friendly pest management techniques are required to increase rice crop productivity and improve its quality (Tudi et al., 2021). It is feasible to develop an alternative to the employment of electrical technologies, such as those used to extract earthworms, to control bloodworms. The use of these electrical devices does not pollute the soil (Görres and Amador, 2021).

In Egypt, most rice cultivated area re exposed to bloodworms as a result of using agricultural drainage water for irrigation that contains higher salinity percentage due to the lack of irrigation water (Elmoghazy and Elshenawy, 2018). Bloodworms infect commonly rice fields that are mechanically transplanted (Elmoghazy and Elshenawy, 2018). Bloodworms moving in the seedling roots spread throughout the fields, resulting in significant crop losses and degradation of grain quality.

In addition, bloodworms lead to difficulty in harvesting using combine harvesters. The infection with bloodworms leads to the formation of elevated parts of the soil that lead to cutting the rubber tracks, breaking the knives, and damaging the transmission gears in the rice combine harvesters (Dumitru et al., 2020). In order to stop the spread of bloodworms, rice fields must be sterilized and treated using effective techniques. Electrical control techniques for pests are considered efficient and secure for crops, soil, and humans (Risley et al., 2016).

The objective of this research is developing a solar-powered device for bloodworm and larvae control in rice fields.

2 Materials and methods

2.1 Experimental site

The solar bloodworm control device was tested at the Al-Serw Agricultural Research Station, Agriculture Research Center, Damietta Governorate, Egypt, which is located at 31.24° N, 31.80° E, during 2021 summer season. The total experimental area was 0.09 ha.

2.2 Soil texture and characteristics

According to Carter and Gregorich (2007), the soil mechanical analysis was carried out at soil layer of 0-600 mm from the soil surface. The soil contains 31.80%, 45.09% and 23.11% clay, silt and sand, respectively. The soil texture was clay loam. The soil organic matter content was 1.65%, the soil acidity suspension (*pH*) was 7.36, and the soil electrical conductivity was 1.89 dSm^{-1}.

2.3 Agricultural practices

A broad-grain rice (*Oryza sativa L.*) named *Sakha 101* was mechanically transplanted using a Kubota 8-row transplanter. All other agricultural practices were applied according to the recommendations of Rice Research and Training Center (2021).

2.4 Solar-powered control device

The device is developed to control bloodworms, which are common pests in rice fields. The device is designed to be easy to move when cultivating rice by the seedling method using a rice transplanter, as

shown in Figure 1. The device is used to control bloodworms and larvae inside rice field sub-soils. The device can be utilized with or without irrigation water covering the cultivated rice fields. The device uses solar energy as a safe and non-polluting energy source. As shown in Figure 1, the device consists of the following components:

2.4.1 Frame

The frame of 6 kg weight was manufactured from galvanized iron pipes with a diameter of 12.7 mm to resist rust and suite the work the flooded rice fields. The frame has been painted with electrical insulating paint to avoid the risk of electric shock. The height of the frame is 1200 mm in length and 300 mm in width, and it is equipped with a semi-circle shaped hinged base with a diameter of 300 mm. The hinged base is straightened and folded when it is moved from one place to another. The frame was lined with 3 mm-thick wood pads to install and isolate the electrical parts, as shown in Figure 1. Two solid rubber wheels with a diameter of 120 mm, which equipped with self-lubricating internal bearings, that are installed on a shaft with a diameter of 10 mm (Figure 3). A front support was installed in the frame at a height of 110 mm above the soil surface to stabilize the device and prevent it from deviating (Figure 1).

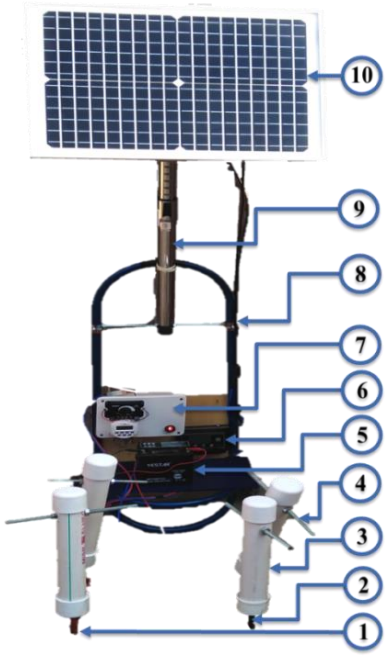

1- positive penetration electrode; 2- negative penetration electrode; 3- electrical current tube; 4- installation handle; 5- DC battery (12 V& 5 A); 6- solar charger; 7- electronic control box; 8- frame; 9- telescopic stand; 10- solar panel 20 W

Figure1 Solar-powered bloodworm control device

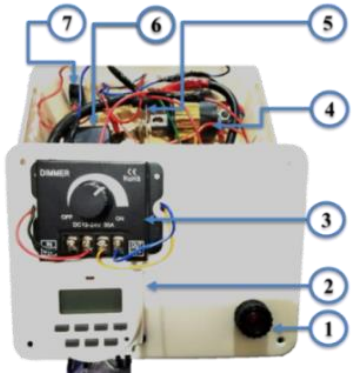

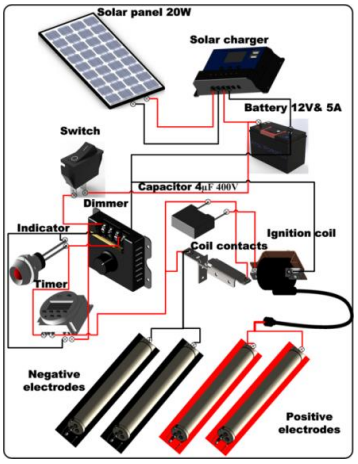

1- indicator lamp; 2- DC programed timer; 3- dimmer; 4- ignition coil; 5- coil contacts; 6- capacitor (4 μf& 400V); 7- device switch

Figure 2 The electronic control box

2.4.2. Solar panel

The used solar panel specifications are listed in Table 1. The area of the solar panel was determined by calculating all electrical loads. As shown in Figure 1, the solar panel was installed using a stainless steel telescopic stand. The diameter of the telescopic stand is 35 mm, and its length when closed is 750 mm; when it extends to its maximum length, it reaches 1100 mm. A pair of hinges is installed behind the solar panel attached to the top of the telescoping stand to adjust the panel to the angle of solar radiation. A smart-controlled solar charger with USB slots, model PWM-20 amps, was used to connect the solar panel, as shown in Figure 1 No. 6. The smart charger automatically recognizes the battery voltage. The solar charger is equipped with a bright LCD screen that shows the percentage of battery charge and the input and output charging status of the controller. The

solar charger is equipped with buttons to reverse the voltage and protect the device from overloads, overcharging, and electrical locks. A dry battery of the DC type with 12 volts and 5 amps was used to suit the loads used and store energy to operate the device (Figure 1, No. 5). The solar-powered unit generates electrical power when exposed to light through the cover glass before opening the terminal junction box.

Table 1 Solar panel specification

Model	HBG20-12M	maximum power (W)	20
Voltage at open circuit (V)	22.32	Open circuit current (A)	1.22
Voltage at maximum power point (V)	18	Current at maximum power (A)	1.11
Power tolerance (%)	±3	Width (mm)	360
Maximum system voltage (V)	1000	Length (mm)	490

2.4.3 Electrical control box

The electrical control box generates a massive electrocution voltage up to 20 kV, which exterminates bloodworms under the soil surface, as shown in Figure 2 and Figure 1, No. 7. The electrical control box consists of a polyethylene box with a length of 200 mm and a width of 120 mm, and it is installed on a pad of wood to isolate it, as shown in Figure 1 No. 7. When opening the power button in Figure 2, No. 7, the positive current reaches the ignition coil, Figure 2, No. 4. The ignition coil is an electrical component that contains two coils, one of which is the primary one that raises the voltage from 12 volts to 220 volts. The secondary coil increases the voltage by 1:100, which raises the potential voltage to 20 kV with an intermittent system. The ignition coil's outlet electrical potential is connected indirectly to the terminals of the contact coil (Figure 2, No. 5). As a result of this indirect contact between one of the terminals of the ignition coil, an internal magnetic field is generated that attracts one of the contact terminals, which generates a continuous electric spark (electrical arc).

The electric spark is transmitted after its intensification by a capacitor (Figure 2, No. 6) with a capacity of 4 μF and 400 V to the positive terminal of the contact coil. During the transfer of the electrical current to the positive electrodes, there is a dimmer that controls the intensity of the current connected to the electrodes to choose the required level of electrocution potential, as shown in Figure 2, No. 3, and Figure 4. The dimmer is connected to an indicator lamp (Figure 2, No. 1), where the intensity of its illumination is directly proportional to turning the dimmer reel in a clockwise direction and vice versa. The dimmer has four ranges to reduce the flow of electrical current, which leads to control the outlet electrocution potential levels from 8 to 20 kV. After determining the current intensity using a dimmer, the electric current is transmitted to a programmed timer (12 V DC) with 16 programs to set the operating period for the electric electrocution circuit (Figure 2, No. 2). The timer can be easily programmed during the day to determine the number of runs and the length of each period, as shown in the electrical circuit in Figure 4. After setting the timer, the positive current is transmitted to the positive electrodes (Figure 1, No. 1). The negative (ground) electrode is connected to the negative electrodes (Figure 1, No. 2).

2.4.4 Isolated electrocution electrodes

There are four electrodes for electrocution, two positive and the other two negative, as shown in Figure 1, No. 1 and 2. Each electrode consists of a polyethylene-insulated tube with a thickness of 5 mm, a diameter of 50.8 mm, and a length of 350 mm. Each electrode is equipped with a handy handle that is pressed to penetrate the soil easily, as shown in Figures 1 and 4. Upper and lower covers were placed on each electrode tube. A hole was drilled in the bottom cover of each electrode to install a solid iron shaft connected to an internally isolated electrocution conduction cable. The length of the internal solid shaft connected to the electrode is 250 mm, and its diameter is 10 mm. Every solid shaft has a tapered end for easy penetration of the soil at the required depth for the control process, as shown in isometric Figure 3. Each positive electrode works with a negative electrode to form a shocking electric circuit

that affects adult bloodworms and larvae. Electrocution beneath the soil layers results in the direct eradication of bloodworms. The continuation of the electrocution, which agitates the worms' nerve cells, causes them to flee to the soil surface, far from rice roots, where they are quickly killed by the electrocution current.

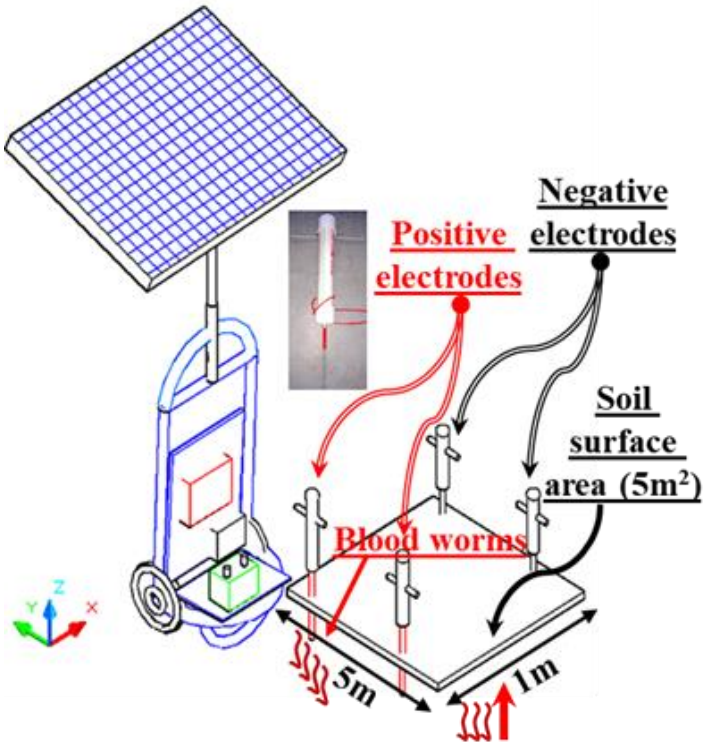

Figure 3 Isometric view of the bloodworm control device's operation

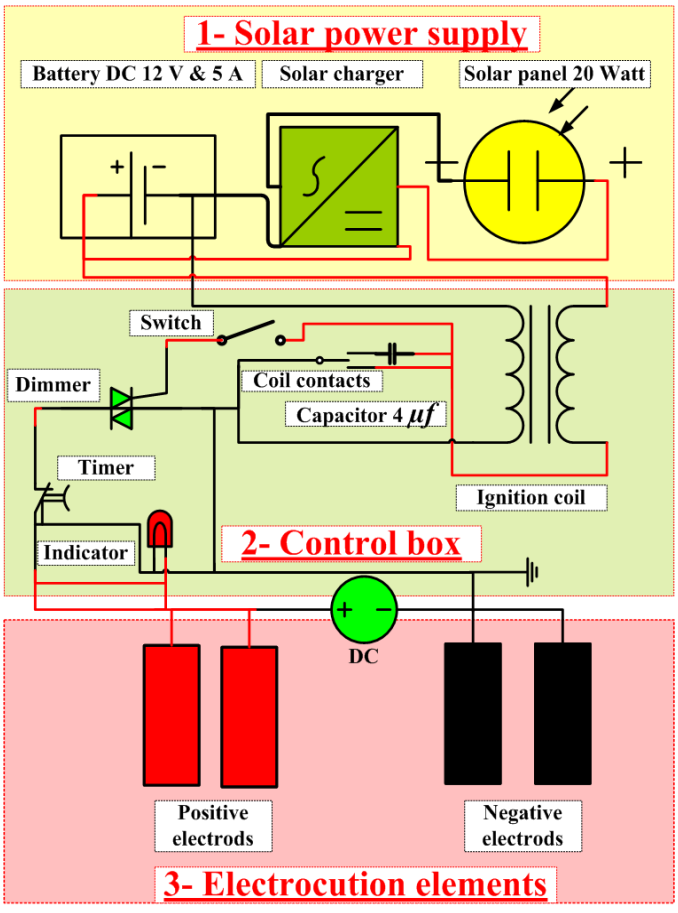

Figure 4 The bloodworm control device's electrical circuit diagram

2.4.5 Treatments

At all the study duration, the following treatments were tested:

1. Electrocution potential: It was tested at levels of 8, 12, 16, and 20 kV.

2. Electrode depth: It was tested at levels of 60, 120, and 180 mm.

3. Controlling period: It was tested at levels of 10, 20, and 30 minutes.

These treatments were compared with traditional bloodworm method using chemical pesticide *Furadan* granules (10% of 14.29 kg ha^{-1}).

2.6 Statistical design

The field experiment was statistically designed as a factorial experiment at complete randomized blocks. The total number of experimental plots was 180. The area of each experimental plot was 5 m^2. The total experimental area was 0.09 ha. Each experimental plot contained five rows of rice seedlings planted at 20-cm spacing's. The control plots have the same area and planting specifications as the experimental plots.

2.7 Measurements

2.7.1 Population of adult and larvae bloodworms

Laboratory experiments were conducted on random soil samples infested with larvae and adult bloodworms using the device. The live adult bloodworms population was collected and counted before treatment using a pitfall trap, a water pan trap, and an insect net. Also, the live larvae were collected from the bottom mud using mud scrapers and scoop samplers and counted after washing with tap water and sieving using a fine screen net (250 µm pore) before treatment (Saha, 2020). As well, the dead adult worms and larvae above the surface of irrigation water after the electrical treatment were collected and counted using the water fine screen net.

2.7.2 Bloodworms reduction percent

It was determined according to Yang et al. (2021) as follows:

$$DR = \frac{No.1 - No.2}{No.1} \times 100 \ \ \% \quad (1)$$

Where: *DR* is the reduction percent of pests, %; *No.1* is the total number of pests before treatment; *No.2*is the total number of pests after treatment.

2.7.3 Bloodworms control efficiency

It was determined according to Yang et al. (2021) as follows:

$$\eta_C = \frac{DR_1 - DR_2}{100 - DR_2} \times 100\ \% \quad (2)$$

Where: η_C is the pest control efficiency, %; DR_1 is the reduction percent of pests in the treatment area, %; DR_2 is the reduction percent of pests in the control area.

2.7.4 Solar-powered control device energy consumption

The consumed energy of the solar pest control device was determined according to Culpin (1986) as follows:

$$Prototype\ consumed\ energy, (kWh\ ha^{-1}) = \frac{\left(\frac{VI}{1000}\right) kw}{Field\ capacity\ ha\ h^{-1}} \quad (3)$$

2.7.5 Consumed solar energy

The consumed solar energy was determined using the global solar, according to Kohak et al. (2019) as follows:

$$Consumed\ solar\ energy, (kWh) = A \times r \times H \times Pr \quad (4)$$

2.7.6 Rice grain yield

Across each plot, three randomized samples of 1 m^{-2} area were taken. The threshed grains were weighted. Then, the grain weight was estimated at 14% moisture content (d.b.).

2.7.7 Solar-powered operating costs

The device operating cost was determined according to Oida (1997).

$$Prototype\ operating\ cost, (USD\ ha^{-1}) = \frac{Device\ hourly\ cost,\ \ (USD)}{Actual\ field\ capacity,\ \ (ha\ h^{-1})} \quad (5)$$

Where: *V* is the potential difference, V; *I is* electrical current intensity, Ampere; *A* is the solar panel area, cm^2; *r is the* solar panel efficiency, %; *H* is annual average radiation (shaded not including); *Pr* is the performance ratio (constant 0.75).

The solar panel's average annual solar energy output is 45.88 kW h. The device consumed between

40 and 100 kWh ha^{-1}. The maintenance cost for the bloodworm control device equals 50 USD annually. The actual field capacity of the bloodworm control device was 0.003 ha h^{-1}. The low productivity of the device is due to the small size of the experimental primary device, which can be increased in scale based on the achieved results and recommendations.

2.8 Statistical analysis:

The statistical programs SPSS (version 2020) and CoStat (version 2019) were used to analyze the recorded data for measurements under the tested variables (Oida, 1997). The mean values and the standard deviation for measurements were estimated using the CoStat program. The significance level was set at a probability of ($p \leq 0.01$), and the analysis of variance (ANOVA) and least significant difference (LSD) tests were also conducted. The effects on the levels of the tested factors and their interactions were studied using linear and stepwise regression analysis.

3 Results and discussion

3.1 Adult and larvae bloodworms population

The laboratory pre-experimental use of the device on bloodworm populations led to the direct electrocution of larvae and bloodworms when the electrocution intensity was increased. The boneless bloodworm body's exterior muscles and skins were dehydrated according to electrocution. The laboratory examination of the survival blood worms after the electrical treatment showed that the bloodworms stopped spawning due to their central nervous system tissues being damaged. The rate of emergence of bloodworms was significantly decreased due to the use of the device.

Data in Table 2 show that the electrical control methodology is more effective in exterminating adult and larvae bloodworms than chemical pesticides using *Furadan*.

After electrical treatment, the mean population numbers of bloodworms and larvae were significantly lowered. The maximum increment percent of exterminating bloodworms and larvae in the electrically controlled plots was 51.8% to 49.67%, respectively, more than the pesticide control plots when using E of 20 kV and E of 180 mm at T of 30 min.

3.2 Bloodworm reduction percent and control efficiency

Figure 5 showed that there is a direct proportion between the levels of applied electrocution intensity and the reduction rate in the bloodworm population that is positively related with the depth of the electrodes and the period of the treatments. As shown in Figure 5a the lowest values of reduction percent in adult and larval bloodworms were 51.35% and 52.80%, respectively, at (*E*) 8 kV and (*D*) 60 mm. The highest reduction percent (*DR*) in adult and larval bloodworms were 93.70% and 95.37%, respectively, at the highest level of electrocution intensity (*E*) of 20 kV and the greatest electrode depth (*D*) of 180 mm. After just one day of treatment, the values of the reduction percent (*DR*) in the population of adult bloodworms and larvae for control treatments utilizing chemical pesticides dropped to 45.16% and 48%, respectively, as shown in Figure 5.

The maximum *DR* values were 90.29% and 91.94% for adult worms and larvae, respectively, at the highest value of (*D*) 20 kV and at the maximum treatment period (*T*) of 30 min. The lowest *DR* values were 54.53% and 55.98% for adult bloodworms and larvae, respectively. The control treatment using the pesticide recorded a reduction in the population of adult bloodworms and larvae by 45.6% and 48%, respectively. Figure 6 shows a direct positive relationship between the electrocution potential (*E*), pest control efficiency at electrode depths (*D*), and the treatment period (*T*). The higher the *D* values, the higher the pest control efficiency values, and vice versa.

Figure 6 clearly demonstrated that the electric control device was more effective and highly significant in exterminating larvae than adult bloodworms. The highest obtained values of pest control efficiency for adult bloodworms and larvae were 88.52% and 91.10%, respectively, at the maximum value of *E* 20 kV and the maximum

electrode depth *D* 180 mm. The lowest values of η_C were 11.29% and 9.24% at *E* 8 kV and *D* 60 mm, respectively, for adult bloodworms and larvae (Figure 6a). Figure 6b depicts the relationship between best control efficiency (η_C) and electrocution potential (*E*) at various treatment periods. The maximum obtained levels of η_C were 82.30% and 84.51%, respectively, for adult bloodworms and larvae at *E* 20 kV and *T* 30 min. The lowest values obtained for η_C for adult bloodworms and larvae were 17.09% and 15.35%, respectively, at the lowest value of *E* 8 kV and the lowest value of *T*, which is 10 min.

As shown in Table 3, linear regression Equations 6-13 were estimated for the interaction between the levels of the tested factors of the solar bloodworm control device. There are two types of linear regression equations: the first is estimated by the input method, while the second is estimated by the stepwise regression method. The stepwise regression method highlights the most significant factors by reducing the interaction between the variables. All levels of the factors individually or the interaction between them showed very high significance in the analysis of variance test (ANOVA) at a probability of $p \leq 0.01$. The determination factor, coefficient of variation, and least significant differences at level 0.01 for the reduction percent and pest control efficiency for the adult bloodworms and larvae, respectively, were listed in Table 3.

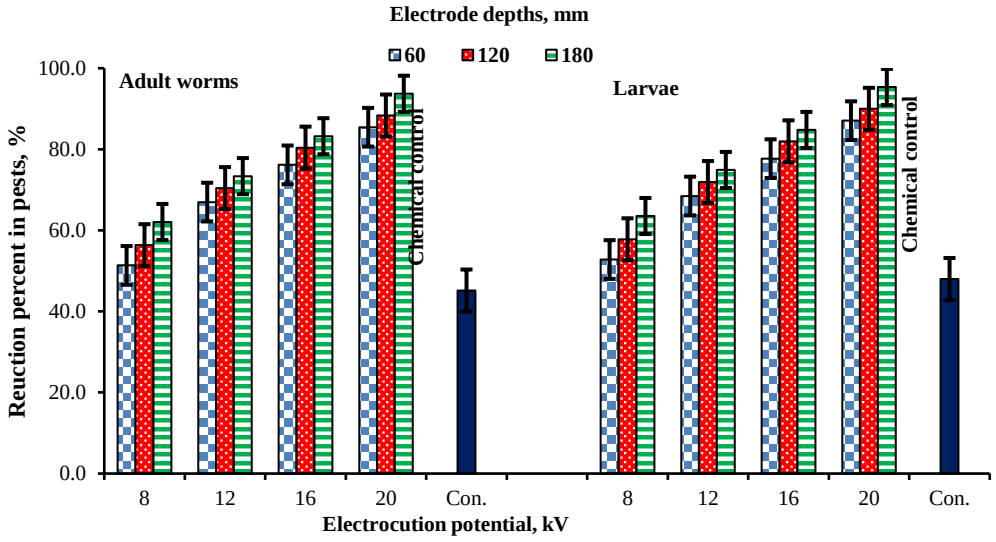

(a) Electrode depths

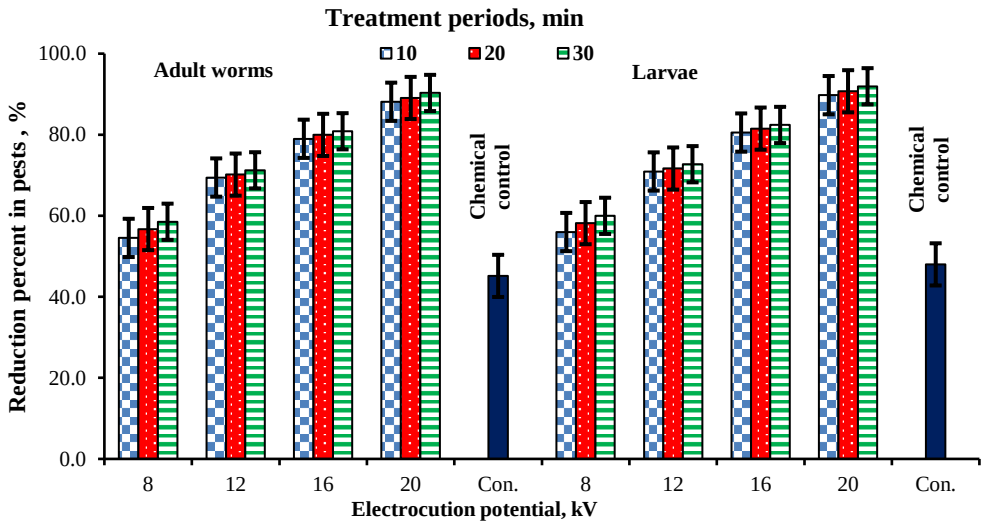

(b) Treatment periods

Figure 5 Effect of electrocution potentials on electrode depths and treatment periods on the reduction percent in adult blood worms and larvae

There are significant differences in the population of adult bloodworms and larvae before and after treatment with an electrocution device over the chemically treated control with *Furadan*, demonstrating the device's effectiveness in reducing the number of worms. The solar-powered pest control device used to exterminate bloodworms outperformed the use of pesticides as a result of its use of a direct electrical elimination methodology. As the use of the pesticide generates acquired autoimmunity that makes pests able to adapt and survive, there is a constant need to produce modified pesticides that are stronger in effect, in agreement with the results of the study by Liu et al. (2014). The solar-powered bloodworm control device recorded a high level of effectiveness in controlling adult bloodworms and their larvae by gradually raising the levels of electrocution potential. The worms' nerve cells are directly stimulated by increasing degrees of electrocution, which causes them to emerge from the mud over the soil surface. During the exit of the worms, electrodes implanted at different depths work to stun the worms and cause their death directly, in agreement with the results of Risley et al. (2016). The maximum electrode depth of 180 mm achieved the best results in reducing the population of bloodworms and larvae. The deeper the electrodes are inserted, the more of the bloodworm and larvae population surrounding rice seedlings will be electrocuted, in line with Saha (2020). Bloodworms, on the other hand, feed on the roots of rice seedlings in fields, multiply quickly, and secrete toxic substances that inhibit growth. The use of a time period of up to 30 minutes achieved maximum efficiency in pest control, and that time is very short compared to treatments using chemical pesticides.

Table 2 Adult and larval bloodworm population and standard deviations before and after electrical and chemical pest treatments

Factors	Adult m^{-2}		Larvae m^{-2}	
Electrocution (*E*), kV	*T1* Mean	*T2* Mean	*T1* Mean	*T2* Mean
8	32 ± 1^{a}	11 ± 2^{a}	25 ± 1^{a}	8 ± 2^{a}
12	31 ± 2^{b}	8 ± 1^{b}	22 ± 1^{b}	6 ± 1^{b}
16	28 ± 1^{c}	6 ± 1^{c}	21 ± 1^{c}	4 ± 1^{c}
20	25 ± 1^{d}	3 ± 2^{d}	20 ± 2^{d}	2 ± 2^{d}
P value	0.0***	0.0***	0.0***	0.0***
LSD 0.01	0.098	0.196	0.139	0.155
Electrode depths (D), mm	*T1* Mean	*T2* Mean	*T1* Mean	*T2* Mean
60	30 ± 6^{a}	8 ± 6^{a}	23 ± 3^{a}	6 ± 4^{a}
120	29 ± 5^{b}	7 ± 5^{b}	22 ± 4^{b}	5 ± 5^{b}
180	29 ± 5^{c}	6 ± 6^{c}	22 ± 5^{c}	4 ± 5^{c}
P value	0.0***	0.0***	0.0***	0.0***
LSD 0.01	0.085	0.17	0.12	0.134
Treatment periods (T), min	*T1* Mean	*T2* Mean	*T1* Mean	*T2* Mean
10	29 ± 6^{a}	7 ± 6^{a}	22 ± 3^{a}	5 ± 5^{a}
20	29 ± 5^{a}	7 ± 6^{a}	22 ± 4^{ab}	5 ± 4^{b}
30	29 ± 5^{b}	7 ± 6^{b}	22 ± 4^{b}	5 ± 5^{c}
P value	0.0***	0.0***	0.0***	0.0***
LSD 0.01	0.085	0.17	0.12	0.134
Chemical control, *Con.*	31±5	17±3	25±4	13±3

Where: E: the electrocution potential, kV; D: the electrode depths, mm; T: the treatment periods, min; T1: the number of bloodworms and larvae before the electrical treatment (Exp. Plot); T2: the number of bloodworms and larvae after the electrical treatment (Exp. Plot); Con.: the chemical treatment (control plots); P: probability significantly ($p \leqslant 0.01$); LSD: least significant differences. a-b the means with no common superscript within each column differed significantly ($p \leqslant 0.01$).

3.3 Rice grain yield

The maximum rice grain yield that was treated using the developed control device achieved 9.2 ton ha^{-1}. While, the average productivity of the chemically treated control treatment decreased to 6.9 ton ha^{-1}, as listed in Table 4. The rice grain yield increased significantly for the treated plots due to the direct extermination of bloodworms that feed on the roots of the crop, and thus the plant completely absorbed the nutrients present in the soil without any

parasites.

3.4 Solar-powered control device operational costs

The operating cost for the device ranged from 25 to 40 USD ha^{-1}. The control treatment with *Furadan* 10% granules costs 75 to 100 USD ha^{-1}, as listed in Table 4. The electrical control methodology reduced the costs of managing bloodworms by 60% to 66.67%. The cost of operating the bloodworm control device is about 10 \$ h^{-1}, which varies according to the degree of infestation and operating time. The device requires annual maintenance costs for batteries of about 20 \$. The investigated bloodworm control device reduced the cost of control because it depends on clean energy, which is solar energy. The device reduces the need for expensive chemical pesticides, which could be adulterated and lead to the destruction of the crop. Pesticides use specific precautions and doses; noncompliance with these negatively impacts the crop, according to Weiss et al. (2022).

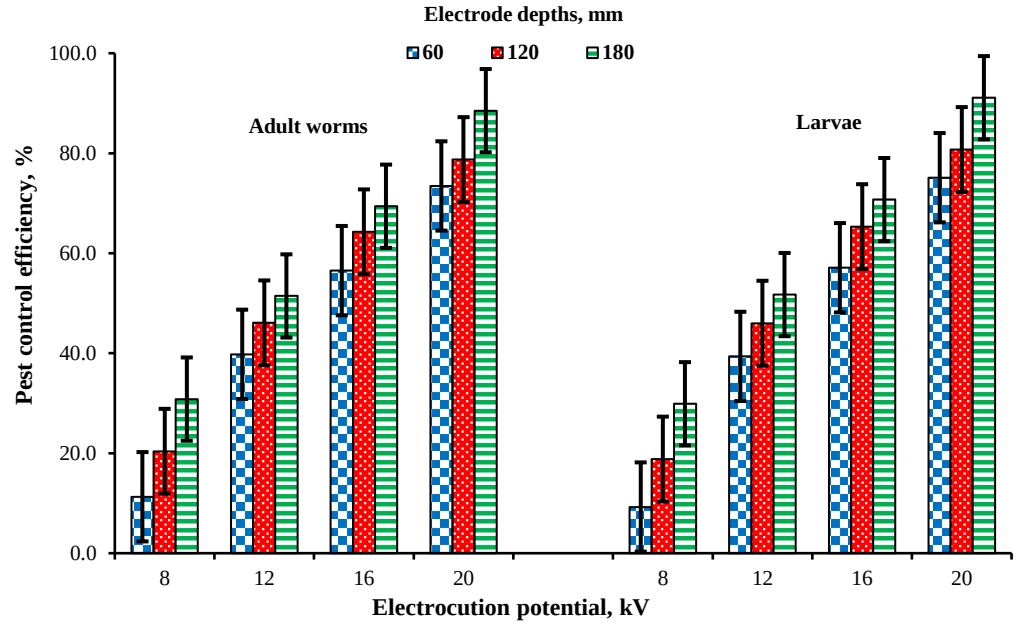

(a) Electrode depths

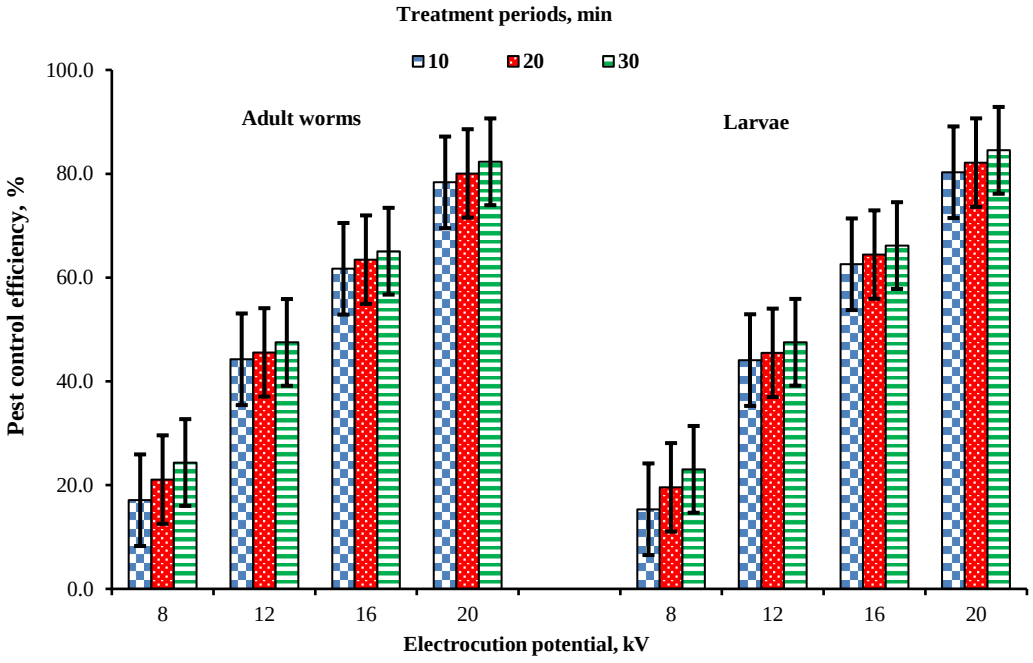

(b) Treatment periods

Figure 6 Effect of electrocution potentials on electrode depths and treatment periods on pest control efficiency in adult blood worms and larvae

Table 3 Regression equations and statistical values for the pest control solar-powered device

Regression equations	R^2	$p < 0.01$ E * D * T	C.V.	LSD 0.01 E * D * T
DR (adult) = 25.841+ 2.685 E + 0.058 D + 0.122 T (6) Or = 36.398 + 2.685 E (stepwise method) (7)	0.897	0.0001 ***	0.870	1.392
DR (Larvae) = 27.121 + 2.700 E + 0.058 D + 0.0123 T (8) Or = 37.726 + 2.700 E (stepwise method) (9)	0.895	0.0001 ***	0.853	1.392
η_C (adult) = -35. 232+ 4.896 E + 0. 123 D + 0.223 T (10) Or = -15.979 + 4.896 E (stepwise method) (11)	0.799	0.0001 ***	2.234	2.537
η_C (Larvae) = -40.145 + 5.192 E + 0.131 D + 0.237 T (12) Or = -19.758 + 5.192 E (stepwise method) (13)	0.798	0.0001 ***	2.342	2.677

Where: *DR*: reduction percent in pests, %; η_C: pest control efficiency, %; *E*: the electrocution potential, kV; *D*: the electrode depths, mm; *T*: the treatment periods, min; *E* * *D* * *T*: the interaction between the tested factors levels; R^2: determination factor; *P*: probability significant ≤ 0.01; *C.V.*: coefficient of variation; *LSD*: at level (0.01), the least significant differences between the mean average and the interaction between the tested factors.

Table 4 Rice grain yield and the solar-powered control device operational costs

Factors Electrocution (*E*), kV	Rice grain yield Ton ha^{-1}	Operational costs USD ha^{-1}
8	6.68±0.56^{a}	25.00±1.72^{a}
12	8.25±0.32^{b}	28.71±1.13^{b}
16	9.15±0.361^{c}	36.66±1.39^{c}
20	9.20±0.42^{d}	40.00±1.84^{d}
P value	0.0***	0.0***
LSD 0.01	0.053	0.184
Electrode depths (D), mm	Mean	Mean
60	8.22±1.48^{a}	31.09±9.39^{a}
120	8.67±1.41^{b}	32.72±9.36^{b}
180	9.16±1.39^{c}	34.51±9.62^{c}
P value	0.0***	0.0***
LSD 0.01	0.046	0.159
Treatment periods (T), min	Mean	Mean
10	8.54±1.51^{a}	32.27±9.60^{a}
20	8.68±1.47^{b}	32.76±9.54^{ab}
30	8.83±1.44^{c}	33.28±9.52^{b}
P value	0.0***	0.0***
LSD 0.01	0.046	0.159
Chemical control, *Con.*	6.90±0.25	75±25

Where: *E*: the electrocution potential, kV; *D*: the electrode depths, mm; *Con.*: the chemical treatment (control plots); *P*: probability significantly ($P \leq 0.01$); *LSD*: least significant differences. $^{a-b}$: the means with no common superscript within each column differed significantly (P ≤ 0.01).

4 Conclusion

The average rice yield productivity of treated plots with the developed bloodworm control device increased to 9.2 ton ha^{-1}. Populations of adult bloodworms and larvae of *Chironomus spp*. have been significantly reduced using the solar-powered control device more than the chemically managed control plots using *Furadan* 10% granular. The highest reduction percent in bloodworm and larval populations was achieved when using the maximal level of electrocution of 20 kV at the deepest electrode depth of 180 mm with the longest treatment period of 30 minutes. The *Furadan* 10% granular control treatment demonstrated a minimum level of pest reduction percent in adult bloodworms and larvae populations, with the lowest percent of 45.16% and 48%, while these percent were 90.92% and 91.94%, respectively, by using a developed control device. The actual field capacity was 0.003 ha h^{-1} for the developed device. The new clean methodology to control bloodworms reduced the costs of managing bloodworms by 60% to 66.67% compared to the chemical one. The operational factors that achieved

higher results were 20 kV for electrocution at the deepest electrode depth of 180 mm and the longest treatment period of 30 minutes. It is recommended to use the solar-powered bloodworm control device in rice fields to exterminate bloodworm infection rather than using chemical pesticides with harmful residual effects on human health and the environment.

Conflict of Interest

The authors declare that they have no conflict of interest.

Acknowledgment

The authors extend their thanks and appreciation to the Agricultural Engineering Research Institute (*AEnRI*), the Agricultural Research Center (*ARC*), the Egyptian Ministry of Agriculture and Land Reclamation for providing support, advice, and technical assistance.

References

Carter, M. R., and E. G. Gregorich. 2007. *Soil Sampling and Methods of Analysis*. 2nd ed. Soil Sampling Designs: Taylor and Francis Group, CRC Press.

Culpin, C. 1986. *Farm Machinery*. 11th ed. Granada Pub. Ltd. London ELBS Collins: 276 – 285.

Dumitru, O. M., S. Iorga, N. V. Vlădut, and C. Brăcăcescu. 2020. Food losses in primary cereal production. A review. *INMATEH-Agricultural Engineering*, 62(3)*:*133-142.

Elmoghazy, A. M., and M. M. Elshenawy. 2018. Sustainable cultivation of rice in Egypt. In *Sustainability of Agricultural Environment in Egypt: Part I*, eds A. M. Negm, and M. Abu-hashim, ch. 6, 119-144. Soil-water-food nexus: Springer Nature.

Görres, J. H., and J. A. Amador. 2021. The soil fauna. In *Principles and Applications of Soil Microbiology*, 3nd ed, eds. T. J. Gentry, J. J. Fuhrmann, and D. A. Zuberer, ch. 8, 191-212. The soil fauna: Elsevier. Science Direct.

Gudeta, K., J. M. Julka, A. Kumar, A. Bhagat, and A. Kumari. 2021. Vermiwash: An agent of disease and pest control in soil, a review. *Heliyon*, 7(3): E06434.

Hegazy, F. E. Z. H., E. A. Hendawy, I. I. Mesbah, and F. A. Salem. 2021. The insect pests, the associated predatory insects and prevailing spiders in rice fields. *Journal of Plant Protection and Pathology*, 12(5): 365-371.

Kamara, B. O. 2015. Quality seed and rice production in Sierra Leone: An assessment of the challenges faced by smallholder rice farmers. M.S. thesis, Pan African Institute of Development, Buea, Cameroon.

Kohak, P. G., R. A. Kandake, V. P. Patekar, and D. S. Ghorpade. 2019. A review on design and fabrication of a solar roadways. *International Research Journal of Engineering and Technology*, 6(9): 2049-2054.

Liu, J., J. Shen, Y. Li, Y. Su, T. Ge, D. L. Jones, and J. Wu. 2014. Effects of biochar amendment on the net greenhouse gas emission and greenhouse gas intensity in a Chinese double rice cropping system. *European Journal of Soil Biology*, 65: 30-39.

Montauban, C., M. Mas, O. S. Wangensteen, V. S. I. Monteys, D. G. Fornós, X. F. Mola, and A. López-Baucells. 2021. Bats as natural samplers: First record of the invasive pest rice water weevil *Lissorhoptrus oryzophilus* in the Iberian Peninsula. *Crop Protection*, 141: 105427.

Oida, A. 1997. Using personal computer for agricultural machinery management. *Kyoto University. Japan, Jica Pub. Smith, HP 1976. Farm Machinery and Equipment*, 1997, 5.

Rice Research and Training Center (RRTC). 2021. Technical recommendations for rice crop. Agricultural Research Center, Egypt: RRTC.

Risley, M. G., S. P. Kelly, K. Jia, B. Grill, and K. Dawson-Scully. 2016. Modulating behavior in C. Elegans using electroshock and antiepileptic drugs. *PLoS One*, 11(9): e0163786.

Saha, D. 2020. Chironomid (*diptera: chironomidae*) deformities as indicator of pollution stress in rice fields of Hooghly district. *Science Explore*, 1(1): 1-9.

Sarwar, M. 2020. Typical flies: Natural history, lifestyle and diversity of Diptera. In *Life Cycle and Development of Diptera*, ed. M. Sarwar, ch. 1, 1-66: IntechOpen.

Savary, S., L. Willocquet, S. J. Pethybridge, P. Esker, N. McRoberts, and A. Nelson. 2019. The global burden of pathogens and pests on major food crops. *Nature Ecology & Evolution*, 3(3): 430-439.

Shaheen, S. M., V. Antoniadis, M. Shahid, Y. Yang, H. Abdelrahman, T. Zhang, N. E. E. Hassan, I. Bibi, N. K. Niazi, S. A. Younis, M. Almazroui, Y. F. Tsang, A. K. Sarmah, K. H. Kim, and J. Rinklebe. 2022. Sustainable applications of rice feedstock in agro-environmental and construction sectors: a global perspective. *Renewable and Sustainable Energy Reviews*, 153: 111791.

Stevens, M. M., P. A. Hughes, and J. Mo. 2013. Evaluation of a commercial *Bacillus thuringiensis* var. *israelensis* formulation for the control of chironomid midge larvae (Diptera: Chironomidae) in establishing rice crops in

south-eastern Australia. *Journal of Invertebrate Pathology*, 112(1): 9-15.

Tudi, M., H. Daniel Ruan, L. Wang, J. Lyu, R. Sadler, D. Connell, C. Chu, and D. T. Phung. 2021. Agriculture development, pesticide application and its impact on the environment. *International Journal of Environmental Research and Public Health*, 18(3): 1112.

Weiss, F. T., C. Ruepert, S. Echeverría-Sáenz, R. I. L. Eggen, and C. Stamm. 2022. Agricultural pesticides pose a continuous ecotoxicological risk to aquatic organisms in a tropical horticulture catchment. *Environmental Advances*, 11: 100339.

Yang, L., S. Wang, R. Wang, Q. Zheng, Q. Ma, S. Huang, and Z. Zhang. 2021. Floating chitosan-alginate microspheres loaded with chlorantraniliprole effectively control *Chilo suppressalis* (Walker) and *Sesamia inferens* (Walker) in rice fields. *Science of the Total Environment*, 783: 147088.